Control of Structure in Multicompartment Micelles by Blending μ-ABC Star Terpolymers with AB Diblock Copolymers

Zhibo Li,[†] Marc A. Hillmyer,*[,†] and Timothy P. Lodge*[,†,‡]

Department of Chemistry and Department of Chemical Engineering and Materials Science, University of Minnesota, Minneapolis, Minnesota 55455

Received October 11, 2005; Revised Manuscript Received November 22, 2005

ABSTRACT: A unique multicompartment micelle, herein referred to as a "hamburger" micelle, was formed from a binary mixture of spherical micelles, formed from polyethylethylene-*b*-poly(ethylene oxide) (EO) diblock copolymers, and segmented wormlike micelles, formed from μ-(polyethylethylene)(poly(ethylene oxide))-(polyperfluoropropylene oxide) (μ-EOF) mikto-arm star terpolymers. Cryogenic transmission electron microscopy (cryoTEM) and dynamic light scattering (DLS) were used to characterize the evolution of micelle structure and size distribution as a function of annealing time, over the course of several months. Considering the extremely low critical micelle concentration of these amphiphilic copolymers, we propose that the micelle evolution was due to a collision/fusion/fission process. The long segmented wormlike micelles first fused with EO spherical micelles, followed by fission to progressively shorter micelles, which finally evolved into more stable hamburger micelles. Three elementary "reactions" were used to describe these structural transitions. Multiple fusions of spherical micelles into already formed hamburger micelles sometimes resulted in the formation of asymmetric hamburger micelles and also induced a micelle shape change from prolatelike to more oblatelike ellipsoids. A binary blend of μ-EOF miko-arm star terpolymer with EO diblock in the bulk prior to micellization did not generate new intermediate micelle structures, presumably because of phase separation between μ-EOF and EO during the film-casting process.

Introduction

The concept of multicompartment micelles—self-assembled aggregates with solvophobic cores that are further subdivided—derives from biological systems, where a single cell incorporates many different units to perform distinct biological functions.[1] Synthetic ABC triblock terpolymers with three mutually immiscible blocks can serve as a minimal model system to create several compartments in one micelle. For example, a hydrophilic block can stabilize the micelle in aqueous media while the other two blocks form segregated domains, which in turn provide distinct chemical environments to store drug molecules, gene therapy agents, or pesticides. In principle, discrete nanocompartments can accommodate two or more incompatible compounds, with the possibility of concurrent transportation and subsequent delivery of various pharmaceutical agents in a desired stoichiometric ratio.[2] Some initial progress toward this goal has recently been made.[2−11] For example, we reported the formation of multicompartment micelles from ABC triblock terpolymers comprising a hydrocarbon, a fluorocarbon, and a water-soluble block.[8−10] For an ABC linear triblock the fluorination of the end A block induced a shape change from a core−corona spherical micelle to a disklike core−shell−corona structure, due to the strong internal segregation between the fluorocarbon (A) and hydrocarbon (B) segments.[8,9] For ABC mikto-arm star terpolymers, the mandatory convergence of the three domains at the molecular junction suppresses the formation of concentric core−shell−corona structures, leading to a fascinating array of new morphologies. As a general packing motif, we have observed disklike fluorocarbon domains sandwiched by two layers of hydrocarbon, while the hydrophilic blocks emanate from the disk/disk interfaces to stabilize the whole micellar core in water. The overall structures that emerge depend on the relative length of the hydrophilic block and can be tuned from discrete multicompartment micelles to extended segmented wormlike micelles with alternating fluorocarbon and hydrocarbon cores.[10]

A common feature among these systems was the coexistence of multiple morphologies, suggesting a lack of global equilibrium during the micellization process. This is not surprising, given the extremely low critical micelle concentrations characteristic of amphiphilic copolymers in general and ones with fluorocarbon blocks in particular. However, it is likely that greater control over micellar shape and size will be desirable in future applications. A promising strategy to tune copolymer structure is blending. In this paper, we explore the formation of multicompartment micelles from binary mixtures of a μ-ABC star terpolymer and an AB diblock copolymer, where the latter is a synthetic intermediate to the mikto-arm star.[12] Specifically, we have mixed dilute aqueous solutions containing, separately, spherical micelles formed from polyethylethylene-*b*-poly(ethylene oxide) (EO) diblocks and segmented wormlike micelles formed from μ-EOF star terpolymers, where F denotes a poly(perfluoropropylene oxide) block. The resulting micellar structure evolution was monitored over several months using cryogenic transmission electron microscopy (cryoTEM) and dynamic light scattering (DLS), as the two micelle types combined to form a common, mixed micellar aggregate structure.

For block copolymers, the exchange dynamics between different micelles are generally more complicated, and much slower, than with conventional surfactants, due to the higher molecular weight. Conventional surfactants follow the principle of closed association and can readily reach thermodynamic equilibrium between micelles and unimers. The exchange dynamics after a perturbation follows the Aniansson−Wall (A−

* Authors for correspondence: hillmyer@chem.umn.edu (M.A.H), lodge@chem.umn.edu (T.P.L.).
[†] Department of Chemistry.
[‡] Department of Chemical Engineering and Materials Science.

10.1021/ma052199b CCC: $33.50
Published on Web 12/21/2005

W) theory, in which the micelle size distribution is adjusted in steps consisting of single chain insertion/expulsion,[13,14] i.e., an evaporation/condensation mechanism. For block copolymer micelles, Halperin and Alexander suggested that the A−W mechanism has the lowest activation energy.[15] On the other hand, Dormidontova compared the free energies between the A−W mechanism and a coalescence mechanism and concluded that the latter becomes remarkably effective when unimer exchange is suppressed.[16] In this work we observe the slow annealing of separate populations of diblock and triblock micelles into one population of mixed micelles and propose that this is accomplished by a collision/fusion/fission process, much more akin to coalescence than evaporation/condensation.

Experimental Section

Materials. Two polyethylethylene-*b*-poly(ethylene oxide) (EO) diblock copolymers, with a hydroxyl group at the block junction, were synthesized by two successive anionic polymerizations; the E block was obtained by catalytic hydrogenation of a 1,2-polybutadiene precursor, prior to initiation of the O block.[17] The mid-hydroxyl functionality was obtained by use of 2-methoxymethoxymethyloxirane as the terminating agent in the butadiene polymerization. The μ-EOF star terpolymers were obtained through a coupling reaction between the mid-hydroxyl-functionalized EO diblock with an acid chloride end-functionalized poly(perfluoropropylene oxide) (F). The detailed synthesis and molecular characterization of the copolymers used here can be found elsewhere.[12] All copolymers have low polydispersities (PDI < 1.2), as determined by size exclusion chromatography (SEC). The polymers are designated as EO($x-y$) and μ-EOF($x-y-z$), where x, y, and z denote the molecular weights in kDa of the E, O, and F blocks, respectively. Two copolymer pairs, μ-EOF(2−6−2)/EO(2−6) and μ-EOF(2−9−2)/EO(2−9), were examined. HPLC grade dichloromethane and deionized water were used as received. The PEE and PFPO blocks have glass transition temperatures of approximately −20[18] and −63 °C,[19] respectively.

Micelle Solution Preparation. All micelle solutions were prepared by direct dispersion of the copolymers into deionized water, to make 1 wt % solutions. All the solutions were stirred in sealed vials at room temperature for at least 1 week before any measurements. The micelle solutions of binary blends were prepared by two different protocols: mixing two different micelle solutions ("postmixing") and, in one instance, mixing two block copolymers before dispersion in water ("premixing"). The former were prepared by combining equal volumes of 1 wt % EO and μ-EOF stock micelle solutions. For the latter a mixture of EO and μ-EOF (1:1, w/w) was dissolved in dichloromethane, slowly dried to form a thin film on the vial wall, and annealed in a vacuum oven for 12 h at 50 °C. The dried blends were then dispersed in water to form 1 wt % micelle solutions and stirred at room temperature. Both the postmixture (2 h after mixing) and premixture (2 weeks after dispersion) solutions were passed through an 0.45 μm microfilter (Millipore) into 0.5 in. diameter optical glass tubes containing a small stirring bar. The glass tube and stirring bar had been rinsed sequentially by HPLC-grade THF and dichloromethane and dried, to prepare dust-free solutions. The solution-containing tubes were sealed by Parafilm to minimize the water loss. The micelle solutions were stirred continuously at a rate of ~2 Hz at room temperature. After different time intervals the size distribution of the micelles was assessed by dynamic light scattering, and an aliquot of solution was extracted for cryoTEM measurements. The annealing time in units of weeks is referenced to the time of mixture formation.

Cryogenic Transmission Electron Microscopy (CryoTEM). CryoTEM samples were prepared in a controlled environment vitrification system,[20] which was saturated with water vapor. All the samples were prepared at room temperature. Typically, a micropipet was used to load a drop of micelle solution (5 μL) onto a lacey supported grid, held by tweezers. The excess solution was blotted with a piece of filter paper, resulting in the formation of thin films of ca. 100−300 nm thickness in the holes. After allowing about 20 s for relaxation, the samples were quickly plunged into a reservoir of liquid ethane at its melting temperature (~90 K) cooled by liquid nitrogen. The vitrified samples were then stored in liquid nitrogen until they were transferred to, and mounted on, a cryogenic sample holder (Gatan 626) and examined with a JEOL 1210 TEM (120 keV) at −178 °C. The phase contrast was enhanced by underfocus. The images were recorded on a Gatan 724 multiscan CCD and processed with DigitalMicrographs version 3.3.1. The ramp-shaped optical density gradients in the background were digitally corrected. In the cryoTEM images shown in this paper, the F domains appear dark and E domains appear gray due to the electron density difference. The O coronas are well solvated with water and normally invisible.

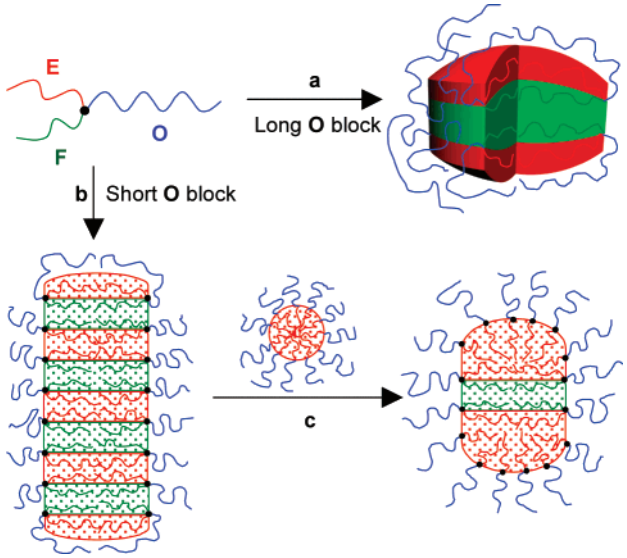

Figure 1. Schematic illustration of the mutlicompartment micelle formation from μ-EOF star terpolymers and binary blends of μ-EOF/EO: (a) hamburger micelle from μ-EOF with a very long PEO block; (b) segmented wormlike micelle from μ-EOF with a short PEO block, (c) hamburger micelle from blends of μ-EOF/EO.

Dynamic Light Scattering (DLS). The samples were investigated using a home-built photometer equipped with an electrically heated silicon oil index-matching bath, a Lexel 75 Ar^+ laser operating at 488 nm, a Brookhaven BI-DS photomultiplier, and a Brookhaven BI-9000 correlator.[21] Intensity autocorrelation functions, $g^{(2)}(t)$, were recorded at room temperature, and the measurements were typically made at angles of 45° and 90°. When the measured and the calculated baselines were in good agreement (difference < 0.1%), the correlation function was accepted. Inverse Laplace transformations were performed using the constrained regularization calculation program REPES[22] to obtain the distribution of relaxation times, which reflect the size distribution of the micelles. The probability-to-reject parameter was maintained at 0.5.

Results

We have previously established the structure and chain packing motif for the micelles formed from μ-EOF star terpolymers in dilute aqueous solution.[10] While keeping the E and F blocks constant, we can tune the micellar structures from discrete species to extended wormlike micelles with segmented cores, as in the illustration shown in Figure 1. When the O block was relatively long, a distinct morphology, referred as to a "hamburger" micelle in this paper, was found to be the dominant structure (path a). In this case the F domain forms the hamburger, with E domains as the "buns" on top of and beneath the F domain. The O blocks emerge from the E/F interfaces and curve around on top and bottom to shield the hydrophobic core. On the other hand, when the O block became too short to shield the whole micelle effectively, several micelle elements

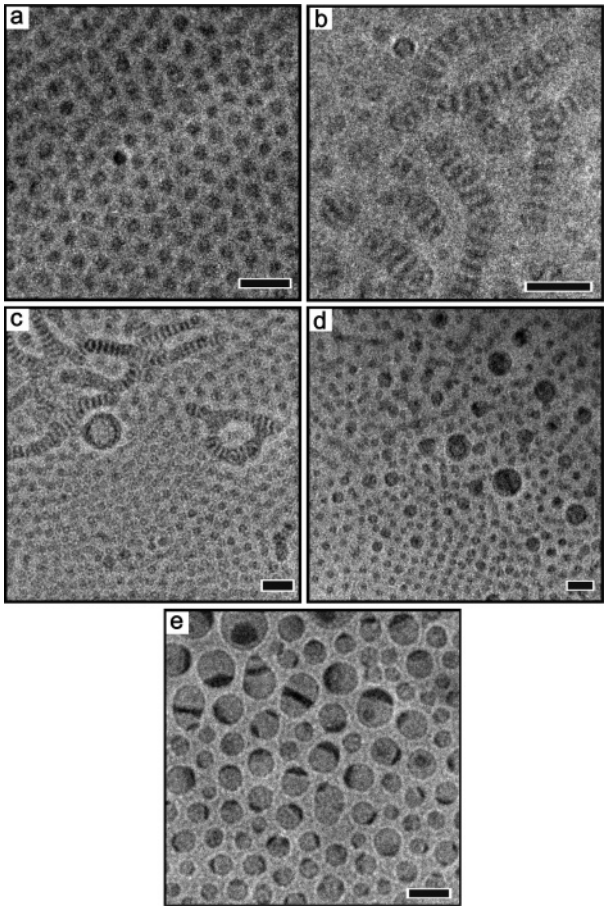

Figure 2. CryoTEM images obtained from a 1 wt % H_2O solution of (a) EO(2−6) diblock, (b) μ-EOF(2−6−2) terpolymer, and postmixture of μ-EOF(2−6−2)/EO(2−6) at (c) week 1, (d) week 9, and (e) week 15. Scale bar indicates 50 nm.

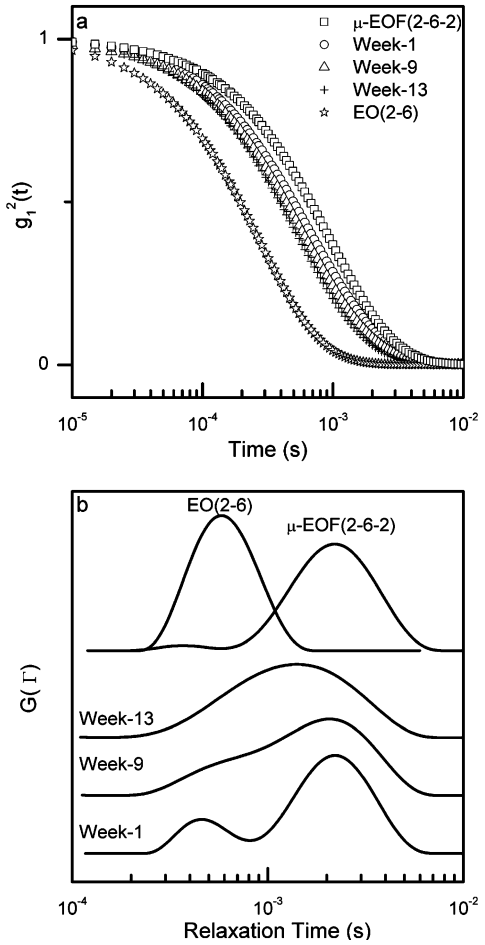

Figure 3. Dynamic light scattering results for the μ-EOF(2−6−2)/EO(2−6) postmixture: (a) correlation functions and (b) distributions of the apparent relaxation times. The scattering angle is 45°.

stacked up "bun-to-bun", to share the O blocks and form a segmented wormlike micelle (path b).

As expected, both EO(2−6) and EO(2−9) diblocks form spherical micelles in dilute aqueous solution with mean hydrodynamic radii of 23 and 24 nm, respectively, from DLS (cumulant analysis). Figure 2a shows a typical cryoTEM image of EO(2−6) prior to postmixing. These spherical micelles adopt an apparent hexagonal packing due to the intermicellar repulsions and geometric confinement; the thickness of the vitrified aqueous film is ca. 100 nm, and no overlap of micelles was observed. The radius of the micellar core is about 7.2 ± 0.5 nm from cryoTEM, which corresponds to aggregation numbers around 420 using the known molecular weight (2 kDa) and density (0.866 g/mL)[23] of the PEE block.

Both star terpolymers, μ-EOF(2−6−2) (Figure 2b) and μ-EOF(2−9−2) (Figure 4a), tend to form segmented wormlike micelles with a broad length distribution. Of the two, μ-EOF(2−6−2) has the shorter O block and forms straight, branched, or even closed (toroidal) segmented wormlike micelles, as the examples shown in Figure 2b and Figure S1 illustrate. The μ-EOF(2−9−2) solutions show similar segmented wormlike micelles, but there is a tendency for the micelles to be shorter and more polydisperse. One week after the solutions of μ-EOF(2−6−2) and EO(2−6) micelles were mixed, the cryoTEM images (examples shown in Figure 2c and Figure S2) displayed the characteristic micelle structures from both μ-EOF(2−6−2) and EO(2−6), i.e., coexistence of segmented wormlike micelles and spherical micelles. Figure 2d and Figure S3 show cryoTEM results of the μ-EOF(2−6−2)/EO(2−6) postmixture after it was

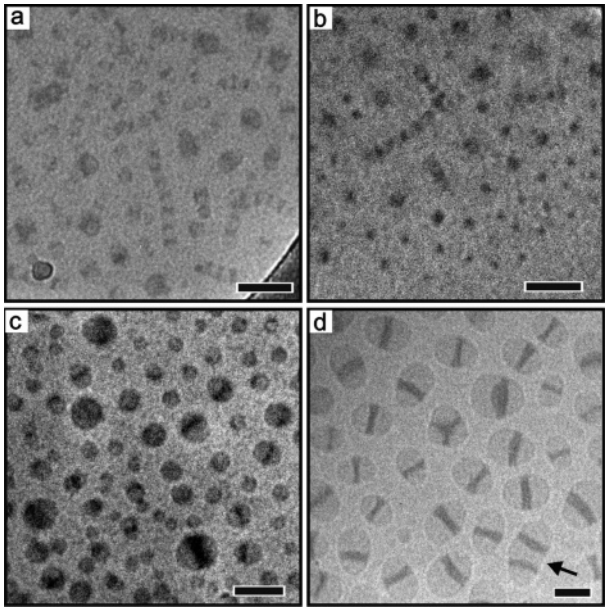

Figure 4. CryoTEM images obtained from a 1 wt % H_2O solution of (a) μ-EF (2−9−2) terpolymer (reproduced from ref 10 with permission) and postmixture of μ-EOF(2−9−2)/EO(2−9) at (b) week 1 and (c, d) week 15. Scale bar indicates 50 nm.

annealed for 9 weeks. Figure 2d reveals a mixture of spherical micelles, shorter segmented cylinders, and irregular hamburger micelles of various sizes. The remarkable change is the disappearance of the long and branched segmented wormlike

micelles, in favor of a mixture with a broad distribution of micelles. As will be discussed subsequently, our proposed explanation for these changes is that the long segmented wormlike micelles break up into smaller fragments due to a process of collision/fusion/fission with EO(2−6) spherical micelles. When the mixture was stirred for another 6 weeks, we observed much more uniform, well-defined hamburger micelles as shown in the cryoTEM images in Figure 2e and Figure S4. The predominant structural features are clearly identified by cryoTEM; the F blocks form a single disk layer (dark regime) while the E blocks form two big bulbs (gray regime) on the top and bottom of the F domain. Thus, each micelle contains an F layer sandwiched by two E domains, which contain the E blocks of μ-EOF and EO. There are also some asymmetric hamburger micelles visible in Figure 2e and Figure S4, i.e., where one E domain is significantly larger than the other. We hypothesize that this asymmetry reflects multiple fusion events between spherical micelles and a single side of an individual hamburger micelle.

Although cryoTEM is an excellent, model-independent technique to explore the micelle nanostructure, it provides limited information about the global properties, such as the macroscopic average micelle size. DLS was thus applied to monitor the relaxation time distribution of the micelles, in synchrony with the cryoTEM measurements. Figure 3 summarizes the DLS results obtained at different aging times for the μ-EOF(2−6−2)/EO(2−6) postmixture at an angle of 45°. Figure 3a compares the squared electric field correlation functions $g_1^2(t)$ vs time, where the mean decay time reflects the average size of micelle aggregates. In Figure 3a it is clear that the postmixture always relaxes more rapidly than pure μ-EOF(2−6−2), but more slowly than pure EO(2−6). Furthermore, the mean relaxation time decreases steadily as the sample is annealed from 1 to 9 to 13 weeks. Thus, even without further analysis we can conclude that the average micelle size decreases with aging time, consistent with the serial cryoTEM images shown in Figure 2. To characterize the overall size evolution, an inverse Laplace transformation (REPES[22]) was performed to obtain the apparent relaxation time distribution. As shown in Figure 3b, pure EO(2−6) has a monomodal distribution of relaxation times (centered near 0.5 ms), while pure μ-EOF(2−6−2) has a rather broad peak centered at a longer relaxation time (ca. 2 ms). The distribution for the postmixture after 1 week has two peaks that can be directly attributed to the coexistence of μ-EOF(2−6−2) and EO(2−6) micelles. By week 9, these two distinct peaks were smeared together, presumably due to the fragmentation of the longer segmented wormlike micelles and the uptake of the spherical micelles. By week 13, the possibly bimodal distribution of week 9 evolved into a broad, monomodal peak centered between the distributions of EO(2−6) and μ-EOF(2−6−2). These slow changes in relaxation time distribution track the micelle size evolution with time and compare favorably with the micelle structure sequence as identified by cryoTEM (Figure 2 and Figures S1−S4).

We also investigated the micelle structural evolution for the postmixture of μ-EOF(2−9−2) and EO(2−9); Figure 4 illustrates typical cryoTEM results. Compared to μ-EOF(2−6−2), μ-EOF(2−9−2) forms relatively shorter segmented cylinders with a broader size distribution, as shown in Figure 4a. In the first week of mixing, Figure 4b displays the superposition of two distinct micelle types from μ-EOF(2−9−2) and EO(2−9). After 15 weeks aging, the hamburger micelle becomes the dominant species with a monomodal distribution. Parts c and d of Figure 4 represent two independent results; both solutions

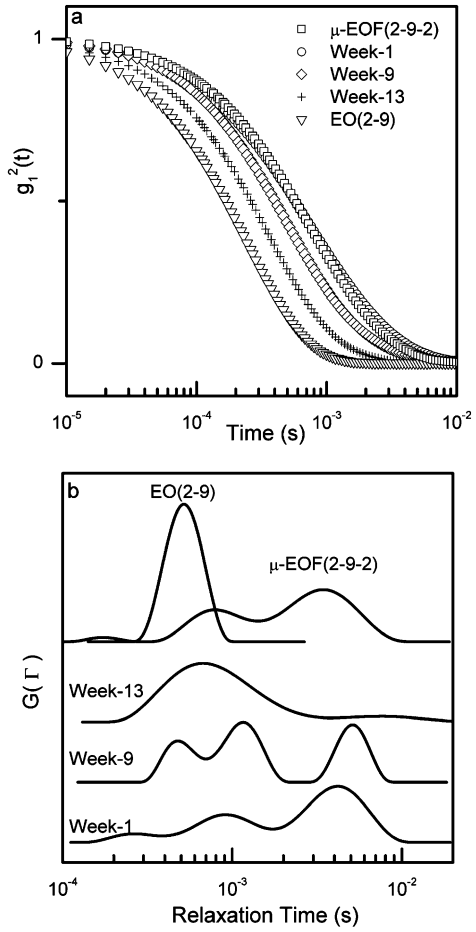

Figure 5. Dynamic light scattering results for the μ-EOF(2−9−2)/EO(2−9) postmixture: (a) correlation functions and (b) distributions of the apparent relaxation times. The scattering angle is 45°.

were made under the same protocol and aged for a comparable time. Figure 5 summarizes the systematic characterization of the micelle size evolution by DLS. The correlation functions (Figure 5a) as well as apparent relaxation time distributions (Figure 5b) display a similar tendency as the postmixture of μ-EOF(2−6−2)/EO(2−6), namely, that the relaxation time of the postmixture lies between that of EO(2−9) and μ-EOF(2−9−2) and diminishes with aging time. For the postmixture of μ-EOF(2−9−2)/EO(2−9) the apparent relaxation time distributions are slightly more complicated than those of the μ-EOF(2−6−2)/EO(2−6) postmixture. The mikto-arm star by itself shows two, and possibly even three, modes in the inversion of the correlation function (Figure 5b). This is consistent with the impression that the μ-EOF(2−9−2) micelles have a rather wide size range (Figure 4a). The distribution overlaps partially with that of EO(2−9). Upon mixing, the distribution also shows three broad peaks reflecting these characteristics. After 9 weeks aging, the population of the largest aggregates is still present, but diminished in relative amplitude, and by week 13 only one, broad mode remains. As with the smaller mikto-arm star and its blends, the DLS (Figure 5) and cryoTEM images (Figure 4 and Figure S5−S7) give a very consistent picture of the overall structural evolution.

In addition to the postmixtures, we also attempted to blend EO(2−6) and μ-EOF(2−6−2) before micelle formation, i.e., a premixture. One might have anticipated that in this way the initial aggregates would contain both diblock and triblocks, thereby rapidly accelerating the convergence to a predominant structure. However, in fact we observed similar micelle sizes

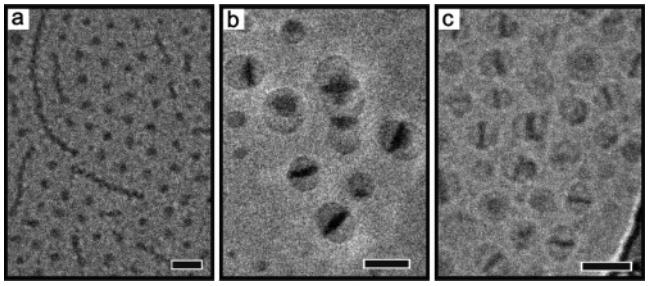

Figure 6. CryoTEM images obtained from a 1 wt % H_2O solution of premixture of μ-EOF(2−6−2)/EO(2−6) at (a) week 3, (b) week 15, and (c) week 25. Scale bar indicates 50 nm.

and structural evolution as with the postmixtures. Figure 6a−c shows cryoTEM images for the premixture of μ-EOF-(2−6−2)/EO(2−6) after aging for 3, 15, and 25 weeks, respectively. Clearly the ultimate micelle morphology of the premixture is same as that of the postmixture, suggesting that indeed the hamburger micelle is the more stable structure. But, Figure 6a reveals a superposition of spherical micelles and segmented wormlike micelles, even after the premixture has been dispersed for 3 weeks. Thus, even when preblended the two copolymers formed separate micelles initially.

Discussion

The results from cryoTEM and DLS presented in Figures 2−6 and in the Supporting Information establish that both postmixtures and premixtures initially contain two types of micelles, which by a very slow process combine to reach a lower free energy state of mixed, multicompartment micelles. CryoTEM provides direct images of the various structures, and DLS tracks the size distribution, as a function of annealing time. The rich variety of micelle structures formed by μ-EOF star terpolymers, which generally featured the "segmented worm" as the predominant local packing motif, was replaced by relatively simple "hamburger" multicompartment micelles, due to combination with the EO spherical micelles. This convergence suggests that the "hamburger" is the more stable morphology in this case. The cartoon in Figure 1 illustrates the proposed chain packing, whereby the diblocks can stabilize a much greater E/O interfacial area than is possible in the triblocks alone and where the high E/F and O/F interfacial tensions preserve the flat F disk. The interesting question then becomes, by what mechanism(s) do the diblock and triblock micelles achieve a common, mixed micelle state?

Thermodynamic equilibrium requires a mechanism of dynamic exchange of polymers among micelles. The exchange dynamics of low molecular weight surfactants can be described by the A−W theory, which assumes that the unimer exchange between surfactant micelles is the dominant factor.[13,14] For diblock copolymer micelles, Halperin and Alexander suggested that the A−W mechanism has the lowest activation energy and would therefore be the preferred equilibration route.[15,24−27] Meanwhile, experimental results have revealed that the exchange dynamics of block copolymer micelles do not necessarily follow the A−W mechanism alone.[28−30] For the micelles formed from poly(acrylic acid)-*b*-poly(methyl methacrylate) (PAA−PMMA) diblock copolymers in water, there was no chain exchange between micelles for copolymers with long PMMA blocks, but a measurable unimer exchange existed for copolymers with shorter PMMA blocks.[31] Micelles formed from a poly(ethylene-*alt*-propylene)-*b*-poly(ethylene oxide) diblock copolymer displayed rapid unimer exchange in DMF but undetectable unimer exchange over the course of weeks in water.[27] Moreover, micelle

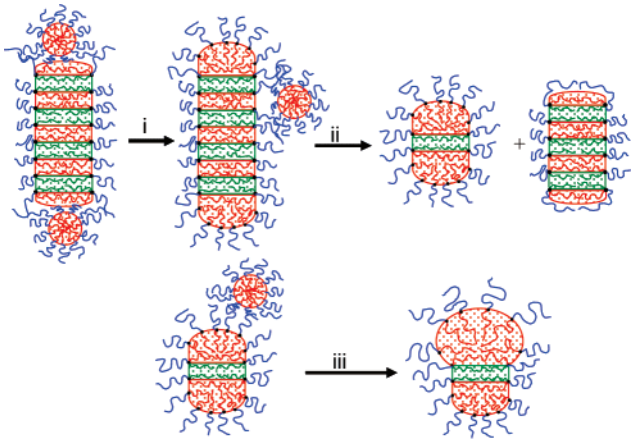

Figure 7. Schematic illustration of the collision/fusion/fission mechanism for the micelle structure evolution.

mixtures formed from 1,2-polybutadiene-*b*-poly(ethylene oxide) (BO) diblock copolymers were demonstrated to be nonergodic, with no unimer exchange observed by a combination of small-angle neutron scattering and cryoTEM measurements.[32,33] Another example to consider concerns spherical micelles formed from poly(ethylene-*alt*-propylene)-*b*-poly(dimethylsiloxane) diblocks in the melt, in which the equilibrium aggregation number decreased, and micelle number density increased, with increasing temperature.[34] The rate of equilibration after a temperature jump was much faster when new spherical micelles were formed upon heating, compared to the situation when micelles dissolved on cooling.[34] After a temperature increase, nucleation of new micelles from existing free chains was complemented by the expulsion of chains from existing micelles and is more rapid than micelle fission. In contrast, upon cooling the increased interfacial energy and chain stretching drive the micelle size to increase, which can only occur with the evaporation of some spheres to release all their chains for growing micelles. The time scale for this process was months, even though single chains could exchange between micelles in seconds.

An alternative equilibration mechanism to consider is the collision/fusion/fission process illustrated schematically in Figure 7, similar to that described by Dormidontova.[16] Three possible "elementary reaction steps" between μ-EOF and EO micelles are envisioned: an EO spherical micelle merges with the hydrophobic end of the segmented wormlike micelle to form a swollen hemispherical end-cap (path i); an EO spherical micelle collides with the body of a segmented cylinder and fuses with the hydrophobic E domain to form a side bulb, which then rapidly breaks the segmented cylinder into two shorter cylinders (path ii); an EO spherical micelle collides with a single hamburger element to form an asymmetric hamburger micelle (path iii). In all cases, the rate-determining step would be the merging of the E cores of the two micelles, as they are screened by the O coronas. Once the E blocks of the spherical micelle were fused with the E domain of μ-EOF micelle, the chains can adjust rapidly because both E and F blocks are in the fluid state at room temperature. Without the complications of either high glass transition temperatures or chain entanglements, the readjustment of E and F blocks should not be the rate-determining step. Subsequently, any intermediate micelles with protrusions on the side disintegrate into two species to decrease the repulsion between corona chains. We infer that path ii predominates in the early stages, due to the higher concentration of micelle "middles" to "end-caps". This conclusion is supported by the cryoTEM results in Figures 2 and 4, where no long segmented

wormlike micelles with more than five repeat elements were observed after the micelle mixtures were aged for 9 weeks. Another factor to consider is that there are more spherical micelles than those formed from μ-EOF star terpolymers, so there can be multiple collisions between spherical micelles and a single hamburger micelle, which could result in the asymmetric hamburger micelles via the mechanism shown as path iii in Figure 7. A significant population of strongly asymmetric hamburger micelles was observed in Figure 2e and Figure 4c,d. Furthermore, the micelle highlighted by an arrow in the bottom right of Figure 4d shows two F disklike cores. The curved interface on one side suggested it is probably an intermediate structure, a "dimer" micelle with two elements. It is reasonable to anticipate that another collision/fusion of an EO spherical micelle at the middle of the dimer will break it into two hamburger micelles.

One initially surprising result is that the premixture did not form different micelle structures from those of postmixtures in the early stages. In a study of binary blends of BO diblock copolymers, there was no unimer exchange for the postmixture, but the premixture produced micelle structures intermediate between the two pristine copolymers.[33] In our experiments, we did not observe significant differences between these two types of mixtures. We attribute this to incompatibility between the components. BO binary blends formed homogeneous solutions in a cosolvent and a single morphology after solvent casting. When this mixture was dispersed into water, both copolymers were incorporated into micelles simultaneously and randomly.[33] In contrast, the mixture of EO(2−6) and μ-EOF(2−6−2) did not form a homogeneous solutions in a cosolvent because the F block shows both hydrophobic and oleophobic properties. Consequently, μ-EOF formed micelles in dichloromethane (by DLS), and distinct diblock and presumably triblock phases exist in the bulk after removing the cosolvent. When the μ-EOF-(2−6−2)/EO(2−6) premixture was dispersed in water, the EO diblock copolymers formed spherical micelles more readily than μ-EOF terpolymers. For example, EO(2−6) or EO(2−9) forms a clear bluish solution in about 24 h. On the other hand, the μ-EOF terpolymers need several days to disperse into a homogeneous micelle solution. Thus, we conclude that the "premixed" state was not mixed at the molecular level.

Another interesting issue to address is the micelle shape and associated chain packing motif. We previously proposed a chain-packing motif for the segmented wormlike micelles, whereby oblate disklike F and E cores were alternately stacked along the axis of a cylinder and O chains emanate from the E/F interfaces to protect the whole micelle core, as illustrated in Figure 1. On the molecular level, the dimension of each disk in a segmented cylinder is limited by the chain length of the F or E blocks. The fully extended F and E blocks are about 5 and 8 nm, respectively. For μ-EOF(2−9−2), the thickness and radius of oblate disk core are 5−7 nm and 6−7 nm, respectively, consistent with the limitation imposed by the block length. In contrast, the multicompartment hamburger micelles shown in Figures 2e, 4d, and 6c, where the dark and gray regimes correspond to F domains and E domains, respectively, cannot be described by a prolatelike ellipsoid with three major axes ($a > b \approx c$), as the lateral dimensions of the hamburger and buns exceed the fully extended F and E block lengths. Here a is the axis normal to the F domain. Therefore, we hypothesize that the asymmetric ellipsoids ($a > b > c$) are thinner in the "hidden" dimension, c, along the direction of the electron beam. This shape is illustrated in Figure 8, where the parameters a, b, and c describing the dimensions of a micelle core are defined. On

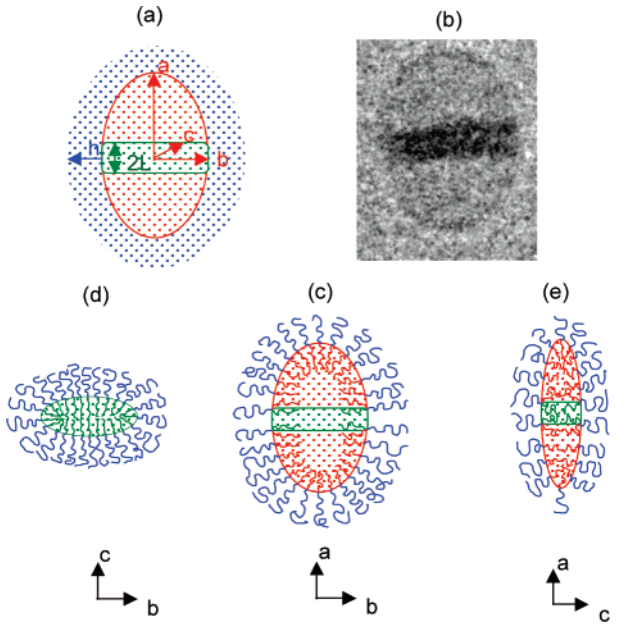

Figure 8. Schematic illustrations of the "hamburger" micelle formed from μ-EOF triblocks plus EO diblocks. (a) Definition of dimensions; hydrocarbon (E) block in red, fluorocarbon (F) block in green, and water-soluble (O) corona in blue. (b) One cryoTEM image of a hamburger micelle, showing the dark F domain and the gray E domains. (c), (d), and (e): cross sections of the micelle along three orthogonal planes, indicating chain packing and relative dimensions.

the basis of the micelles in Figure 4d, the micelle dimensions, i.e., $2a$, $2b$, and $2L$, are 60 ± 7.3 nm, 43 ± 5.5 nm, and 12 ± 3.3 nm, respectively. If we further approximate the thickness of micelle corona (h) to be the rms end-to-end distance of an O block (6.3 nm) and c to be the contour length of the F block (5.2 nm), the radii of the equivalent hard sphere for a prolatelike ellipsoid ($a = 30 \pm 3.7$ nm as major and $b = c = 22 \pm 2.8$ nm as minor axis) and an oblatelike ellipsoid ($b = 22 \pm 2.8$ nm as major axis and $c = 11.5$ nm as minor axis) are 31 and 25 nm, respectively. In contrast, if a geometric average value of experimentally determined values of a and b was adopted for the major axis ($b' = \sqrt{a^*b} = 32$ nm), also with $c = 11.5$ nm, the equivalent hard-sphere radius for oblatelike ellipsoid will be 30 nm. The DLS experimental results (by cumulant analysis) indicated the mean hydrodynamic radius to be 27 nm, which suggested that the oblatelike ellipsoid is a viable candidate to describe the three-dimensional structure of the micelles formed from binary blends of μ-EOF/EO. According to the proposed formation mechanism, the volume of an F domain is preserved between the initial segmented wormlike micelle and final hamburger micelle. Finally, the anisotropic shape depicted in Figure 8 provides an explanation for the absence in Figure 4d of images of micelles viewed from the top, i.e., along the a axis; the blotting process, combined with the confinement to a thin (ca. 100 nm) layer, induces the micelles to lie flat.

Because of the lack of free copolymers chain in the micelle solution, the basic reaction unit for each collision event is a spherical micelle with $R_h \sim 23$ nm. The incorporation of a spherical micelle makes an E domain rather too bulky to be stable with its initial interfacial curvature against the corona, which would require the individual E blocks to be significantly stretched. Therefore, an oblatelike ellipsoid shape was adopted with smaller interfacial curvature to relieve the stretching of E block; the F domains still have the flat interface with water due to very high surface tension.[10] For the oblatelike ellipsoid, both the F and E blocks in some sense formed bilayer structure

however with curved edges.[35] Since the F domain has a constant volume, the interfacial areas between F and H_2O and between F and E are not sensitive to this transition from prolatelike to oblatelike ellipsoid. Furthermore, since both F and E are in a fluid state at room temperature, there is also no kinetic obstacle for the reorientation of F and E blocks from the prolatelike to the oblatelike shape.

Summary

Using a combination of cryoTEM and DLS, we have followed the evolution of multicompartment micelle structure after blending two micelle solutions. Separate solutions of μ-EOF mikto-arm star terpolymers formed segmented wormlike micelles with a broad size distribution, whereas EO diblock copolymers formed spherical micelles with a narrow size distribution. Upon mixing, a very slow annealing process took place over the course of several months, resulting in the formation of mixed "hamburger" micelles, containing a central fluorocarbon disk, surrounded on top and on bottom by hydrocarbon "buns". We propose that the micelle structure evolution follows a collision/fusion/fission mechanism. The long segmented wormlike micelles were first fragmented into shorter micelles due to fusion of EO micelles with E domains, followed by fission into two, shorter worms. Eventually this process led to narrowly distributed hamburger micelles. As a consequence of multiple collision and fusion of spherical micelles on one side of a hamburger micelle, asymmetric multicompartment micelles were also observed. A premixture of triblock and diblock did not generate new intermediate micelle structures but followed the same slow evolution observed in the case of "postmixed" samples. This was attributed to phase separation between μ-EOF and EO during the film formation process. Overall, the most significant result is that binary blending of an μ-EOF terpolymer with an EO diblock copolymer provides a promising strategy to tune the various multicompartment micelle structures and in particular to drive the system to form a unique multicompartment micelle with a significantly narrower size distribution.

Acknowledgment. This work was supported primarily by the MRSEC Program of the National Science Foundation under Award DMR-0212302. Z.L. thanks William Edmonds for fruitful discussion during the manuscript preparation.

Supporting Information Available: Complementary cryoTEM images with larger fields of view for micelle solution mixtures after different aging times (Figures S1-S7). This material is available free of charge via the Internet at http://pubs.acs.org.

References and Notes

(1) Laschewsky, A. *Curr. Opin. Colloid Interface Sci.* **2003**, *8*, 274.
(2) Lodge, T. P.; Rasdal, A.; Li, Z.; Hillmyer, M. A. *J. Am. Chem. Soc.* **2005**, *127*, 17607.
(3) Gohy, J.-F.; Willet, N.; Varshney, S.; Zhang, J.-X.; Jérôme, R. *Angew. Chem., Int. Ed.* **2001**, *40*, 3214.
(4) Erhardt, R.; Boeker, A.; Zettl, H.; Kaya, H.; Pyckhout-Hintzen, W.; Krausch, G.; Abetz, V.; Müeller, A. H. E. *Macromolecules* **2001**, *34*, 1069.
(5) Erhardt, R.; Zhang, M.; Boeker, A.; Zettl, H.; Abetz, C.; Frederik, P.; Krausch, G.; Abetz, V.; Müeller, A. H. E. *J. Am. Chem. Soc.* **2003**, *125*, 3260.
(6) Liu, Y.; Abetz, V.; Müeller, A. H. E. *Macromolecules* **2003**, *36*, 7894.
(7) Lei, L.; Gohy, J.-F.; Willet, N.; Zhang, J.-X.; Varshney, S.; Jérôme, R. *Macromolecules* **2004**, *37*, 1089.
(8) Zhou, Z.; Li, Z.; Ren, Y.; Hillmyer, M. A.; Lodge, T. P. *J. Am. Chem. Soc.* **2003**, *125*, 10182.
(9) Lodge, T. P.; Hillmyer, M. A.; Zhou, Z.; Talmon, Y. *Macromolecules* **2004**, *37*, 6680.
(10) Li, Z.; Kesselman, E.; Talmon, Y.; Hillmyer, M. A.; Lodge, T. P. *Science* **2004**, *306*, 98.
(11) Kubowicz, S.; Baussard, J.-F.; Lutz, J.-F.; Thünemann, A. F.; von Berlepsch, H.; Laschewsky, A. *Angew. Chem., Int. Ed.* **2005**, *44*, 5262.
(12) Li, Z.; Hillmyer, M. A.; Lodge, T. P. *Macromolecules* **2004**, *37*, 8933.
(13) Aniansson, E. A. G.; Wall, S. N. *J. Phys. Chem.* **1974**, *78*, 1024.
(14) Aniansson, E. A. G.; Wall, S. N.; Almgren, M.; Hoffmann, H.; Kielmann, I.; Ulbricht, W.; Zana, R.; Lang, J.; Tondre, C. *J. Phys. Chem.* **1976**, *80*, 905.
(15) Halperin, A.; Alexander, S. *Macromolecules* **1989**, *22*, 2403.
(16) Dormidontova, E. E. *Macromolecules* **1999**, *32*, 7630.
(17) Hillmyer, M. A.; Bates, F. S. *Macromolecules* **1996**, *29*, 6994.
(18) Khandpur, A. K.; Macosko, C. W.; Bates, F. S. *J. Polym. Sci., Part B: Polym. Phys.* **1995**, *33*, 247.
(19) Zhu, S.; Edmonds, W. F.; Hillmyer, M. A.; Lodge, T. P. *J. Polym. Sci., Part B: Polym. Phys.* **2005**, *43*, 3695.
(20) Bellare, J. R.; Davis, H. T.; Scriven, L. E.; Talmon, Y. *J. Electron Microsc.* **1988**, *10*, 87.
(21) Pan, C.; Maurer, W.; Liu, Z.; Lodge, T. P.; Stepanek, P.; von Meerwall, E. D.; Watanabe, H. *Macromolecules* **1995**, *28*, 1643.
(22) Jakes, J. *Collect. Czech. Chem. Commun.* **1995**, *60*, 1781.
(23) Fetters, L. J.; Lohse, D. J.; Richter, D.; Witten, T. A.; Zirkel, A. *Macromolecules* **1994**, *27*, 4639.
(24) Cantú, L.; Corti, M.; Salina, P. *J. Phys. Chem.* **1991**, *95*, 5981.
(25) Smith, C. K.; Liu, G. *Macromolecules* **1996**, *29*, 2060.
(26) Goldmints, I.; Holzwarth, J. F.; Smith, K. A.; Hatton, T. A. *Langmuir* **1997**, *13*, 6130.
(27) Willner, L.; Poppe, A.; Allgaier, J.; Monkenbusch, M.; Richter, D. *Europhys. Lett.* **2001**, *55*, 667.
(28) Wang, Y.; Balaji, R.; Quirk, R. P.; Mattice, W. L. *Polym. Bull. (Berlin)* **1992**, *28*, 333.
(29) Wang, Y.; Kausch, C. M.; Chun, M.; Quirk, R. P.; Mattice, W. L. *Macromolecules* **1995**, *28*, 904.
(30) Esselink, F. J.; Dormidontova, E.; Hadziioannou, G. *Macromolecules* **1998**, *31*, 2925.
(31) Rager, T.; Meyer, W. H.; Wegner, G.; Winnik, M. A. *Macromolecules* **1997**, *30*, 4911.
(32) Won, Y.-Y.; Davis, H. T.; Bates, F. S. *Macromolecules* **2003**, *36*, 953.
(33) Jain, S.; Bates, F. S. *Macromolecules* **2004**, *37*, 1511.
(34) Cavicchi, K. A.; Lodge, T. P. *J. Polym. Sci., Part B: Polym. Phys.* **2003**, *41*, 715.
(35) Zemb, T.; Dubois, M.; Demé, B.; Gulik-Krzywicki, T. *Science* **1999**, *283*, 816.

MA052199B